Available online at www.sciencedirect.com
SCIENCE DIRECT®

Journal of Fluorine Chemistry 125 (2004) 1709–1714

JOURNAL OF FLUORINE CHEMISTRY
www.elsevier.com/locate/fluor

Ternary and tetrahedral symmetry in hybrid fluorides, fluoride carbonates and carbonates

Karim Adil[a], Amor Ben Ali[a], Gilles Dujardin[b], Robert Dhal[b], Marc Leblanc[a,*], Vincent Maisonneuve[a]

[a]*Laboratoire des Oxydes et Fluorures, UMR CNRS 6010, IRIM2F FR CNRS 2575, Faculté des Sciences et Techniques, Université du Maine, Avenue Olivier Messiaen, 72085 Le Mans Cedex 09, France*
[b]*Laboratoire de Chimie Organique et Macromoléculaire, UMR CNRS 6011, IRIM2F FR CNRS 2575, Faculté des Sciences et Techniques, Université du Maine, Avenue Olivier Messiaen, 72085 Le Mans Cedex 09, France*

Received 9 May 2004; received in revised form 30 June 2004; accepted 2 July 2004

Abstract

Tren amine cations and carbonate anions adopt a ternary symmetry while *tetra* amine cations are tetrahedral. The symmetry of these constitutive ions influences strongly the nature of the solids which crystallise from solutions. Large fluorinated aluminate polyanions with tetrahedral symmetry appear in the presence of *tren* amine, while infinite chains of AlF_6 octahedra are observed with *tetra* amine and that noncentrosymmetric structures are frequently encountered in rare earth fluoride carbonates.

Keywords: Hybrid fluorides; Carbonates; Hydrothermal synthesis; Solvothermal synthesis; Microwave heating; Solid state

1. Introduction

It is commonly accepted that the shape and size of amine cations play a significant role on the formation of organically templated microporous solids [1]. Charge density of the protonated amine is supposed to match the charge density of the oligomeric building species. The nature of the structural building units depends on numerous factors such as concentration and nature of the starting materials, the solvent or temperature [2]. Consequently, the prediction of the structures of the crystallised solids is not straightforward; several structures with differing dimensionality (0D–3D) can be obtained with a same templating cation. However, it can be observed that a (pseudo) three-fold symmetry is frequently encountered in microporous oxydes: $AlPO_4$-5 [3], ULM-5 [4], ULM-16 [5], VSB-1 [6], MIL-31 [7]. Cubic symmetry also occurs, for example in cloverite ($Fm\text{-}3c$, $a = 52.712$ Å) [8]. This last phase is obtained with quinuclidinium cations, which present a three-fold symmetry axis. In this paper, it is shown that ternary symmetry of the organic cations favours the formation of large inorganic building anions with a high symmetry. Similarly, a ternary symmetry of inorganic anions favours the formation of structures with high symmetry, eventually acentric. Such trends are encountered in fluoride aluminates, fluoride carbonates and carbonates.

2. Ternary and tetrahedral symmetry in fluoroaluminates

Only one 3D fluorinated inorganic network is reported to date in the fluoride zirconate $(H_3O)\cdot[CN_3H_6]_5\cdot(ZrF_5)_6$ [9] where guanidinium cations present a ternary symmetry. Consequently, guanidine CN_3H_5 (*gua*) and *tris*(aminoethyl)-amine $[N(C_2H_4)NH_2]_3$ (*tren*), which gives also a cation with a three-fold symmetry, were tested in order to promote the crystallisation of open frameworks in fluoride aluminates. An organic cation with a higher symmetry, tetrahedral *tetra*-2-aminomethyl-methane (*tetra*), was also used. All

---

* Corresponding author. Tel.: +33 2 4383 3350; fax: +33 2 4383 3506.
E-mail address: marc.leblanc@univ-lemans.fr (M. Leblanc), vincent.maisonneuve@univ-lemans.fr (V. Maisonneuve).

0022-1139/$ – see front matter
doi:10.1016/j.jfluchem.2004.09.019

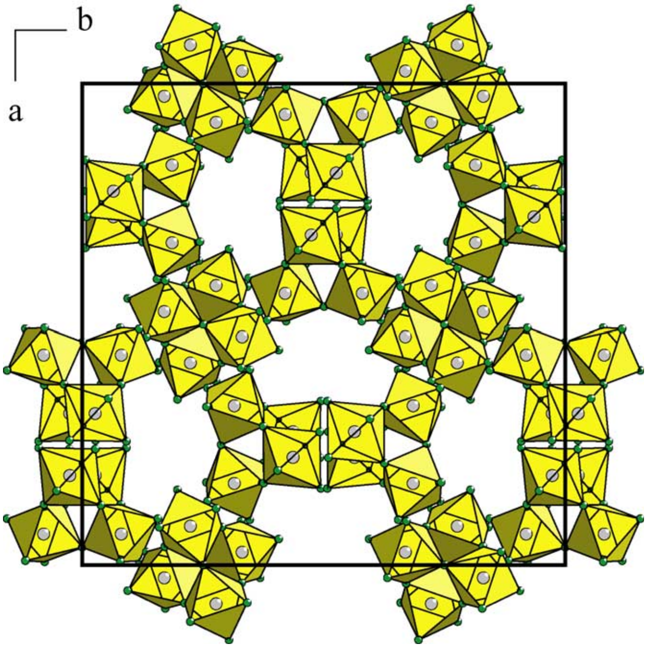

Fig. 1. Isolated $(Al_4F_{18})^{6-}$ units in $(H_3O)_2\cdot[H$*gua*$]_{16}\cdot(Al_4F_{18})_3$.

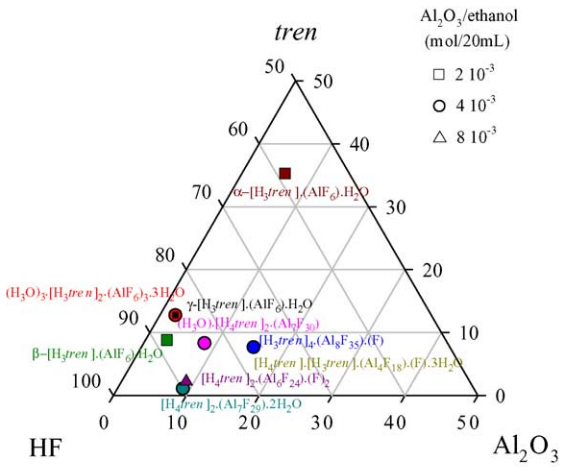

Fig. 2. Crystalline phases obtained in the Al_2O_3–*tris*(aminoethyl)amine–HF–ethanol system.

experiments were performed by solvothermal or hydrothermal synthesis in a microwave oven.

2.1. Guanidinium fluoroaluminates

Few experiments were performed in the Al_2O_3–*gua*–HF–ethanol system at $T = 190\ ^{\circ}C$ during 1 h. One cubic phase is worth to note: $(H_3O)_2\cdot[H$*gua*$]_{16}\cdot(Al_4F_{18})_3$, I-43d, $a = 20.597(2)$ Å, $Z = 12$. The structure is built up from tetrahedral units of AlF_6 octahedra linked by corners (Fig. 1). CN_3 groups of guanidinium cations lie in a plane; however, it is not yet clear if hydrogen atoms are slightly displaced from the mean plane or not. A second phase was found: $(H_3O)\cdot[H$*gua*$]_2\cdot(AlF_6)$ ($C2/m$, $Z = 2$).

2.2. Tris(aminoethyl)ammonium fluoroaluminates

The Al_2O_3–*tren*–HF–ethanol system was investigated over a large range of concentrations of the starting materials at $T = 190\ ^{\circ}C$ during 1 h. In Fig. 2, the compositions of the crystallized phases are indicated and their positions are representative of the ratio of the starting materials for a given Al_2O_3/ethanol ratio.

At high HF and amine concentrations, three forms of $[H_3$*tren*$]\cdot(AlF_6)\cdot H_2O$ are evidenced (α, β, γ [10]), together with $(H_3O)_3\cdot[H_3$*tren*$]_2\cdot(AlF_6)_3\cdot 3H_2O$. The stability of the structures, built up from AlF_6 octahedra and triprotonated amines, is mainly ensured by a network of hydrogen bonds.

At decreasing HF and amine concentrations, it is remarkable that a condensation of the AlF_6 octahedra gradually occurs, leading to the largest polyanions observed in fluorides. $(Al_2F_{10})^{4-}$ anions (dimers of octahedra linked by a F–F edge), $(Al_4F_{18})^{6-}$ (already mentioned for guanidinium fluoroaluminate $(H_3O)_2\cdot[H$*gua*$]_{16}\cdot(Al_4F_{18})_3$), $(Al_8F_{35})^{11-}$ and $(Al_7F_{30})^{9-}$ appear (Fig. 3). Further condensation leads to 1D structures, where ${}_{\infty}(Al_7F_{29})^{8-}$ and ${}_{\infty}(Al_6F_{24})^{6-}$ chains are found (Fig. 4), and finally, to $(Al_2(OH)_{0.5}F_{0.5})_6\cdot H_2O$ [11] pyrochlore or to the hexagonal tungsten bronze type $Al(OH,F)_3\cdot 0.33H_2O$ (HTB) [12]. The corresponding compounds are $[H_4$*tren*$]\cdot(Al_2F_{10})\cdot H_2O$ [10], $[H_3$*tren*$]\cdot[H_4$*tren*$]\cdot(Al_4F_{18})\cdot(F)\cdot 3H_2O$ [10], $[H_3$*tren*$]_4\cdot(Al_8F_{35})\cdot(F)$ [10], $(H_3O)\cdot[H_4$*tren*$]_2\cdot(Al_7F_{30})$ [13], $[H_4$*tren*$]_2\cdot(Al_7F_{29})\cdot 2H_2O$, $[H_4$*tren*$]_2\cdot(Al_6F_{24})\cdot(F)_2$ [10]. It must be noted that other microcrystalline phases are evidenced; their structure determination from powder diffraction data is difficult and is not yet achieved.

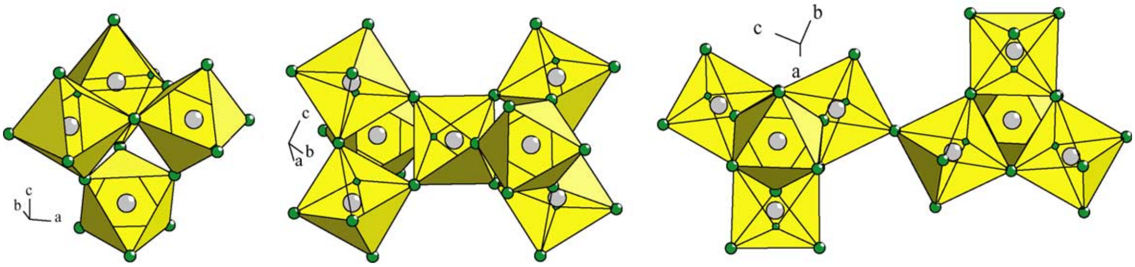

Fig. 3. $(Al_4F_{18})^{6-}$, $(Al_7F_{30})^{9-}$ and $(Al_8F_{35})^{11-}$ units in $[H_3$*tren*$]\cdot[H_4$*tren*$]\cdot(Al_4F_{18})\cdot(F)\cdot 3H_2O$ (left), $(H_3O)\cdot[H_4$*tren*$]_2\cdot(Al_7F_{30})$ (middle) and $[H_3$*tren*$]_4\cdot(Al_8F_{35})\cdot(F)$ (right), respectively.

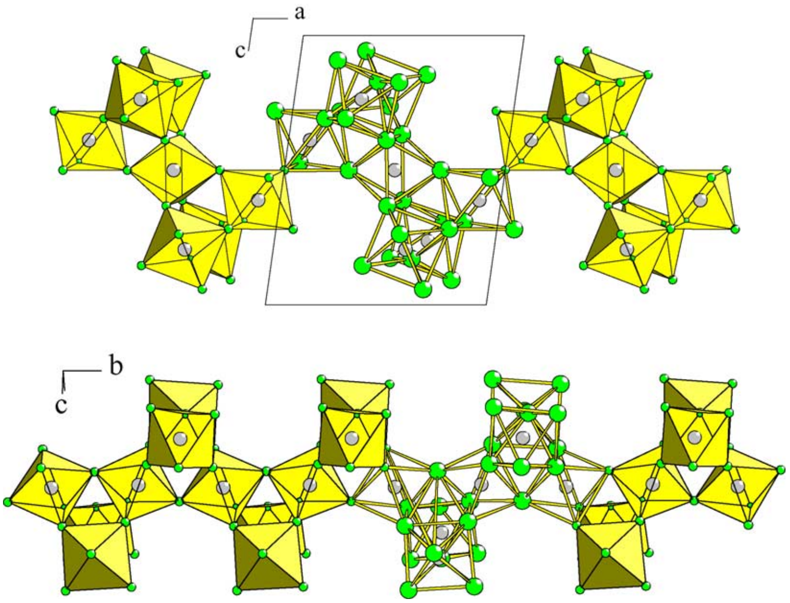

Fig. 4. $_{\infty}(Al_7F_{29})^{8-}$ and $_{\infty}(Al_6F_{24})^{6-}$ chains in $[H_4tren]_2\cdot(Al_7F_{29})\cdot 2H_2O$ (top) and $[H_4tren]_2\cdot(Al_6F_{24})\cdot(F)_2$ (bottom), respectively.

The geometry of the amine cations is strongly correlated with the protonation state. Planar or non planar configurations are found and the distances from central tertiary N_t to external primary N_p nitrogen atoms lie into three groups around 3.0, 3.3 and 3.8 Å (Fig. 5). $[H_3tren]^{3+}$ cations adopt exclusively a ‘‘spider’’ shape with the shortest N_t–N_p distances (2.90–3.02 Å or 3.23–3.33 Å). $[H_4tren]^{4+}$ cations exhibit one short (3.23–3.30 Å) and two long distances (3.63–3.80 Å) or three long distances (3.75–3.86 Å); the corresponding configurations are either planar (non hydrogen atoms lie approximately in a plane) or non planar with a ‘‘scorpion’’ shape (Table 1).

2.3. $[H_4(tetra\text{-}2\text{-}aminomethyl\text{-}methane)]^{4+}$ fluoroaluminates

Infinite chains of *cis* or *trans* connected AlF_6 octahedra are ordered in a body-centred tetragonal arrangement [14] which perfectly fits the tetrahedral symmetry of organic $[H_4tetra]^{4+}$ cations (Fig. 6). In both phases

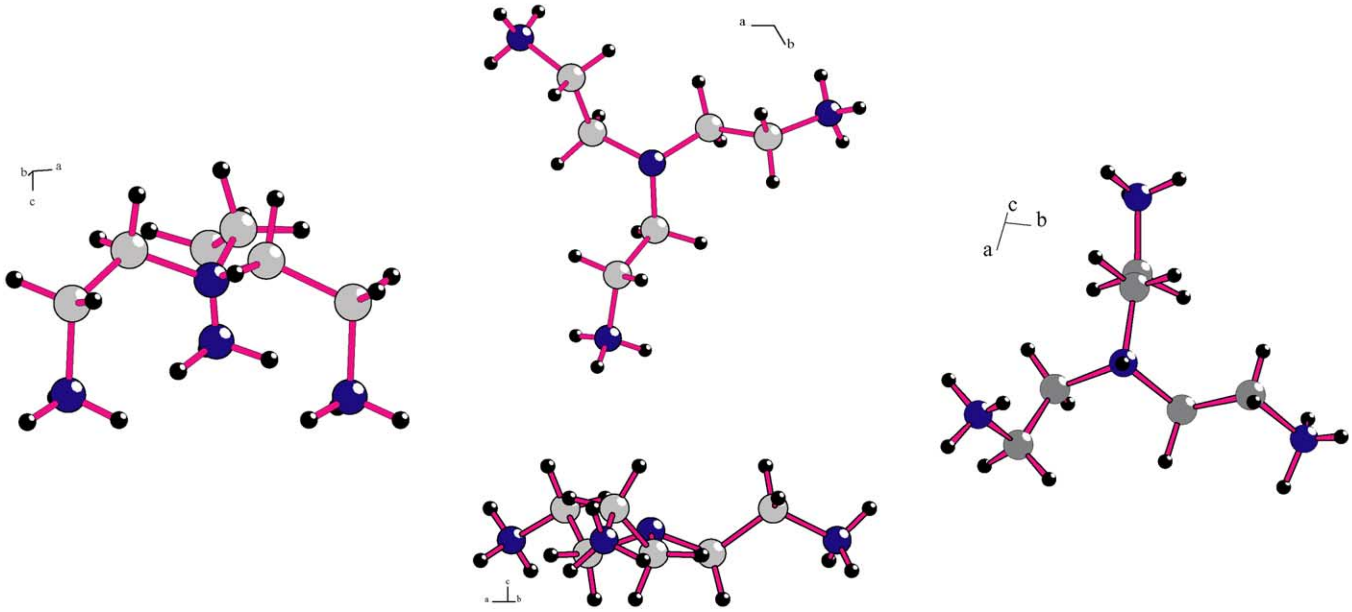

Fig. 5. Configurations of *tren* cations: planar $[H_4tren]^{4+}$ (middle) and non planar $[H_3tren]^{3+}$ ‘‘spider’’ (left) or $[H_4tren]^{4+}$ ‘‘scorpion’’ (right).

Table 1
N_t–N_p distances (Å) from central to external nitrogen atoms in (protonated *tren*) cations

	N_t–N_p distances			$<N_t–N_p>$		
α-[H_3*tren*]·(AlF_6)·H_2O	2.99	3.00	3.01	3.00 ± 0.01	[H_3*tren*]	Spider
β-[H_3*tren*]·(AlF_6)·H_2O	2.99	3.00	3.01	3.00 ± 0.01	[H_3*tren*]	Spider
γ-[H_3*tren*]·(AlF_6)·H_2O		3 × 3.33		3.33 ± 0.01	[H_3*tren*]	Spider
(H_3O)$_3$·[H_3*tren*]$_2$·(AlF_6)$_3$·3H_2O	3.23	3.24	3.29	3.25 ± 0.04	[H_3*tren*]	Spider
	3.23	3.25	3.29	3.26 ± 0.03	[H_3*tren*]	Spider
[H_4*tren*]·(Al_2F_{10})·H_2O	3.29	3.63	3.78		[H_4*tren*]	Scorpion
[H_3*tren*]·[H_4*tren*]·(Al_4F_{18})·(F)·3H_2O		3 × 2.96		2.96 ± 0.01	[H_3*tren*]	Spider
		3 × 3.75		3.75 ± 0.02	[H_4*tren*]	Plane
[H_3*tren*]$_4$·(Al_8F_{35})·(F)	2.90	2.91	3.02	2.94 ± 0.08	[H_3*tren*]	Spider
(H_3O)·[H_4*tren*]$_2$·(Al_7F_{30})	3.23	3.77	3.79		[H_4*tren*]	Scorpion
[H_4*tren*]$_2$·(Al_7F_{29})·2H_2O	3.30	3.77	3.80		[H_4*tren*]	Scorpion
[H_4*tren*]$_2$·(Al_6F_{24})·(F)$_2$	3.72	3.78	3.86	3.79 ± 0.07	[H_4*tren*]	Scorpion
	3.78	3.80	3.85	3.81 ± 0.04	[H_4*tren*]	Scorpion

[H_4*tetra*]·(AlF_5)$_2$, the intra-molecular N–N distances are 5.05 ± 0.03 Å in the (0 0 1) plane; all other N–N distances are 3.66 ± 0.03 Å.

3. Ternary and tetrahedral symmetry in fluoride carbonates and carbonates

The hydrothermal systems Na_2CO_3–LnF_3–H_2O (A = Na, K; Ln = rare earth, Y) are very rich. Five different phases are evidenced either in Na_2CO_3–YbF_3–H_2O [15] or in Na_2CO_3–YF_3–H_2O [16] systems at $T = 190$ °C. With potassium carbonate, three phases are found [17]. The ternary symmetry of carbonate ions favours the formation of a coordination 6 + 3, 3 + 3 + 3 or 6 + 2 of the rare earth cations. The resulting anionic entities share $(CO_3)^{2-}$ ions and build the three-dimensional network in which alkaline cations are inserted. Generally, three carbonate groups, which lie in a plane, surround the metal cation. Infinite layers, with a three-fold symmetry, result from the connection of these $Ln(CO_3)_3$ entities. Non centrosymmetric phases derive from the parallel stacking of such layers.

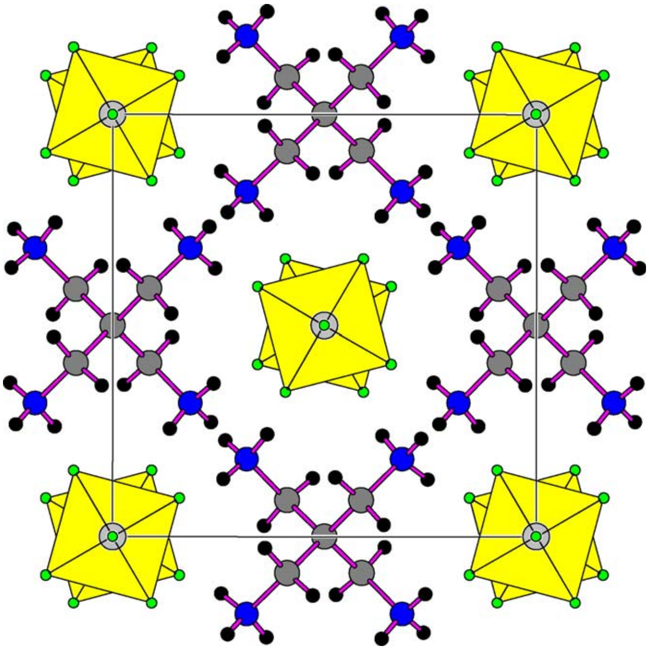

Fig. 6. [0 0 1] projection of the structure of *trans*-[C(CH_2NH_3)$_4$]·(AlF_5)$_2$.

3.1. Rare earth Ln^{III}, Ln^{IV} fluorides

In $K_4Ln_2^{III}(CO_3)_3F_4$ [17], fluoride anions lie above and below the mean plane $Ln(CO_3)_3$ and two polyhedra, linked by a common F–F edge, form a dimer (Fig. 7). In $K_4Ce^{IV}(CO_3)_3O_2{\cdot}2H_2O$ [18], these fluorine atoms are replaced by one peroxide ion, disordered on two equally probable positions (Fig. 7). In $K_4Ce^{IV}(CO_3)_3O{\cdot}2H_2O$ [19], the $Ln(CO_3)_3O_2$ polyhedra are linked by axial opposite oxygen atoms and the resulting infinite chains are separated by alkaline cations.

In $Na_3Ln_2(CO_3)_3F$ [20], three oxygen atoms from three carbonate groups and one fluoride ion complete the

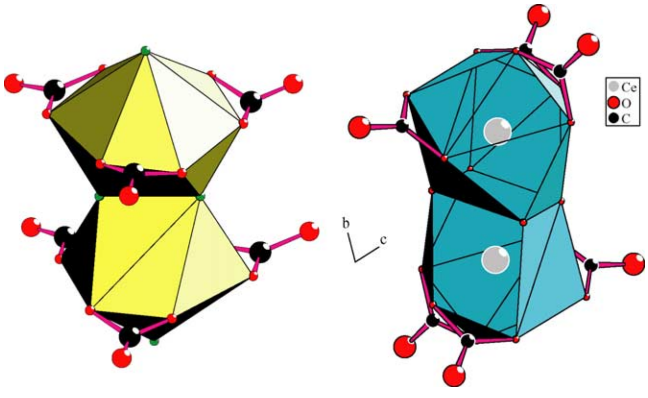

Fig. 7. Dimers of polyhedra in $K_4Ln^{III}{}_2(CO_3)_3F_4$ (left) and $K_4Ce^{IV}(CO_3)_3O_2{\cdot}2H_2O$ (right).

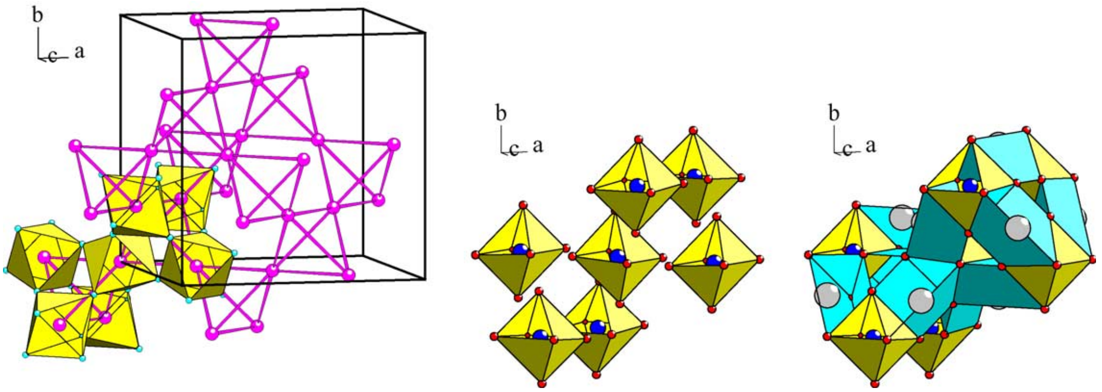

Fig. 9. Comparison of the connection of the AlX_6 octahedra (X = OH, O, F) by corners in the pyrochlore structure of $Al_2(OH,F)_6{\cdot}H_2O$ (left) and by (Na,Ln) polyhedra in $Na_2LiLn(CO_3)_3$ (right). Evidence of the double tetrahedra of AlX_6 octahedra in both structures.

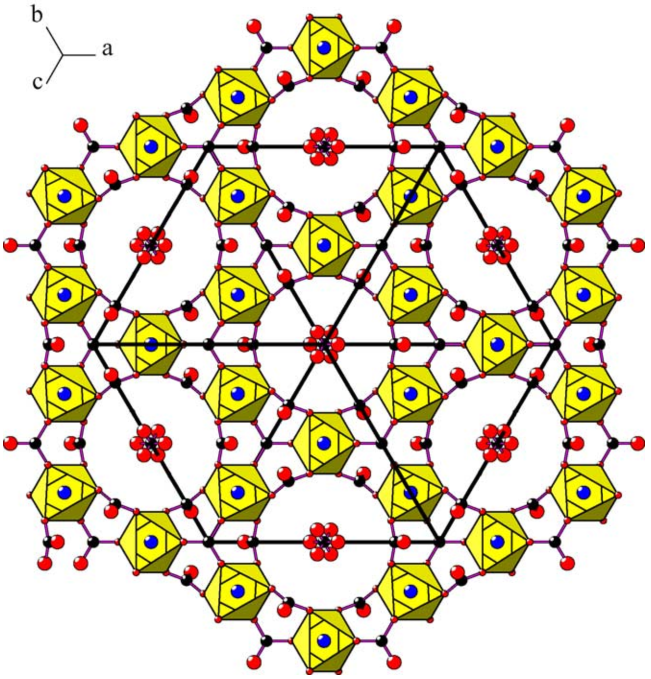

Fig. 8. Hexagonal tungsten bronze (HTB) type layers of LiO_6 octahedra in $Na_2LiLn(CO_3)_3$.

coordination $Ln(CO_3)_3$ polyhedra. Double layers are formed by the connection of dimers built up from two $Ln(CO_3)_3(CO_3)_3F$ polyhedra, linked by one fluoride ion.

3.2. Cubic symmetry in $Na_2LiLn(CO_3)_3$

The addition of lithium carbonate to the preceding Na_2CO_3–LnF_3–H_2O systems strongly affects the crystallization domains. Only one solid phase is found over the whole range of studied compositions: $Na_2LiLn(CO_3)_3$ [21]. In spite of the disorder, which affects both the cation and the anion sub-networks, a cubic symmetry is observed. It is remarkable that Li^+ cations, in 16c sites, occupy the positions of metal cations in the pyrochlore structure and adopt the same octahedral coordination. They build infinite HTB type layers of LiO_6 octahedra connected by carbonate groups (Fig. 8). Moreover, the LiO_6 octahedra are linked by Na^+ or Ln^{3+} cations, disordered on 48f positions, while the MX_6 octahedra are linked by corners in pyrochlore. It is also remarkable that double tetrahedra of octahedra, linked by a common octahedron, are found in the structures of $Al_2(OH,F)_6{\cdot}H_2O$ pyrochlore, $Na_2LiLn(CO_3)_3$ (Fig. 9), $[H_4\textit{tren}]_2{\cdot}(Al_7F_{29}){\cdot}2H_2O$ and $[H_4\textit{tren}]_2{\cdot}(Al_6F_{24}){\cdot}(F)_2$ (Fig. 4).

4. Conclusion

Numerous fluoroaluminates and rare-earth fluoride carbonates or carbonates are compared. It is found than three-fold symmetry of protonated *tren* amine favours the crystallization of fluoroaluminates with large or infinite polyanions. Three-fold symmetry of carbonate anions leads to the formation of $M(CO_3)_3X_n$ entities (M = rare earth Ln^{3+} or 3d transition M^{2+} cations, $X = F^-$, O^{2-}, $(O_2)^{2-}$, $(CO_3)^{2-}$) and to the crystallization of acentric structures. At the opposite, a tetrahedral symmetry of *tetra* amine favours the formation of infinite chains of *cis* or *trans* connected AlF_6 octahedra. These general trends help to design and to test new organic templates, which are currently investigated in order to promote the crystallization of open 3D fluorinated frameworks.

References

[1] G. Férey, Chem. Mat. 13 (2001) 3084–3098.
[2] G. Férey, J. Fluo. Chem. 72 (1995) 187–193.
[3] S.T. Wilson, B.M. Lok, C.A. Messina, T.R. Cannan, E.M. Flanigen, J. Am. Chem. Soc. 104 (1982) 1146–1147.
[4] T. Loiseau, D. Riou, F. Taulelle, G. Férey, in: J. Weitkampf, H.G. Karge, H. Pfeiffer, W. Homderich (Eds.), Zeolites and Related Microporous Materials; State of the Art, 84A, Elsevier, New York, 1994, pp. 395–403.
[5] T. Loiseau, G. Férey, J. Mat. Chem. 6 (1996) 1073–1074.

[6] N. Guillou, Q. Gao, M. Nogues, R.E. Morris, M. Hervieu, G. Férey, A.K. Cheetham, C. R. Acad. Sci. IIc 2 (1999) 387–392.

[7] C. Sassoye, T. Loiseau, F. Taulelle, G. Férey, Chem. Commun. (2000) 943–944.

[8] M. Estermann, L. McCusker, C. Baerlocher, A. Merrouche, H. Kessler, Nature 352 (1991) 320–323.

[9] A.V. Gerasimenko, B.V. Bukvetskii, V.B. Logvinova, R.L. Davidovich, Koord. Khim. 22 (8) (1996) 584–590.

[10] K. Adil, V. Maisonneuve, M. Leblanc, Acta Crystallogr. E60 (2004) m1379–m1381.

[11] J.-L. Fourquet, M. Rivière, A. Le Bail, N. Nygrens, J. Grins, Eur. J. Solid State Inorg. Chem. 25 (1988) 535–540.

[12] A. Le Bail, C. Jacoboni, M. Leblanc, R. De Pape, H. Duroy, J.-L. Fourquet, J. Solid State Chem. 77 (1988) 96–101.

[13] E. Goreshnik, V. Maisonneuve, M. Leblanc, Z. Anorg. Allg. Chem. 628 (2002) 162–166.

[14] K. Adil, E. Goreshnik, S. Courant, G. Dujardin, M. Leblanc, V. Maisonneuve, Solid State Sci., in press.

[15] A. Ben Ali, V. Maisonneuve, M. Leblanc, Solid State Sci. 4 (2002) 1367–1375.

[16] M.O. Awaleh, A. Ben Ali, V. Maisonneuve, M. Leblanc, J. Alloys Compd. 349 (2003) 114–120.

[17] N. Mercier, M. Leblanc, J. Durand, Eur. J. Solid State Inorg. Chem. 34 (1997) 241–249.

[18] J.C. Barnes, C.S. Blyth, Inorg. Chim. Acta 110 (1985) 133–137.

[19] S. Yonezawa, V. Maisonneuve, J. Marrot, M. Takashima, M. Leblanc, J. Phys. Chem. Solids 62 (2001) 1507–1512.

[20] N. Mercier, F. Taulelle, M. Leblanc, Eur. J. Solid State Inorg. Chem. 30 (1993) 609–617.

[21] A. Ben Ali, V. Maisonneuve S. Houlbert, A. Bulou, G. Silly, J.Y. Buzaré, M. Leblanc, Solid State Sci., in press.